

LLNL-JRNL-402525



LAWRENCE
LIVERMORE
NATIONAL
LABORATORY

Challenging Nuclear Structure Models Through a Microscopic Description of Proton Inelastic Scattering off ^{208}Pb

M. Dupuis, S. Karataglidis, E. Bauge, J.-P.
Delaroche, D. Gogny

March 26, 2008

Physics Letters B

Disclaimer

This document was prepared as an account of work sponsored by an agency of the United States government. Neither the United States government nor Lawrence Livermore National Security, LLC, nor any of their employees makes any warranty, expressed or implied, or assumes any legal liability or responsibility for the accuracy, completeness, or usefulness of any information, apparatus, product, or process disclosed, or represents that its use would not infringe privately owned rights. Reference herein to any specific commercial product, process, or service by trade name, trademark, manufacturer, or otherwise does not necessarily constitute or imply its endorsement, recommendation, or favoring by the United States government or Lawrence Livermore National Security, LLC. The views and opinions of authors expressed herein do not necessarily state or reflect those of the United States government or Lawrence Livermore National Security, LLC, and shall not be used for advertising or product endorsement purposes.

Challenging nuclear structure models through a microscopic description of proton inelastic scattering off ^{208}Pb

M. Dupuis¹ S. Karataglidis² E. Bauge J.-P. Delaroche

Commissariat à l'Énergie Atomique, Centre DAM - Ile de France, Service de Physique Nucléaire, Bruyères-le-Châtel, 91297 Arpajon CEDEX, France

D. Gogny

L-414, Lawrence Livermore National Laboratory, Livermore, CA 94551, USA.

Abstract

A fully microscopic calculation of inelastic proton scattering off ^{208}Pb is presented, and compared to experimental scattering data for incident proton energies between 65 and 201 MeV. By constructing the nucleon-nucleus interaction through the folding of nuclear structure information with a reliable nucleon-nucleon effective interaction that has no adjusted parameter, a consistent framework is built, for probing the influence of different descriptions of nuclear structure on nucleon inelastic scattering predictions. The absence of phenomenological normalization in this framework guarantees a unique and unambiguous interpretation of our calculations in terms of quality of the underlying nuclear structure description: a feature that had been reserved, until recently, to the electron probe. This tool is used to investigate the effect of long range correlations embedded in excited states, on calculated inelastic observables, demonstrating the sensitivity of nucleon scattering predictions to details of the nuclear structure.

Key words:

PACS: 21.60.Jz, 24.10.Ht, 24.10.Eq

In the past, the structure of ground and excited states of stable nuclei has extensively been probed with high energy electron scattering experiments. Since the Coulomb interaction and its treatment in a scattering problem are both very well known, charge ground state and transition densities can be accurately extracted from scattering observables in a model-independent way. Parallely, elastic and inelastic proton scattering have been used to challenge both nuclear structure and in-medium nucleon-nucleon interaction, but disentangling structure

effects from in-medium nuclear interaction effects is not as easy and unambiguous as in the case of electron probe.

Proton inelastic scattering for heavy nuclei has already been modeled within several frameworks, but each of them either includes some phenomenological adjustment for the nucleon-nucleus (NA) interaction or/and the nuclear structure information, or relies on approximations whose effects are not well controlled. First of all, DWBA analyses with the phenomenological collective model have extensively been used and allowed the assignment of nuclei spin and parities of numerous excitations. More recently, inelastic scattering data have been analyzed [1] by using microscopic transition densities from Quasi-particle Random Phase Approximation (QRPA)

¹ Present address: Los Alamos National Laboratory, Los Alamos, New Mexico, USA.

² Present address: Department of Physics and Electronics, Rhodes University, Grahamstown 6140, South Africa.

calculations. However, these analyses still involve several renormalization processes both for the NA interactions and the QRPA transition densities as well as an approximated treatment of the exchange transition amplitude. As a consequence, some ambiguities persist when challenging nuclear structure with proton scattering data since the observed agreement cannot be unambiguously assigned to either effects of the adjustments/approximations or to the intrinsic quality of the underlying nuclear structure model.

However, recent progress in the understanding of nuclear interactions has permitted very precise analysis of nucleon scattering and has allowed to further challenge the quality of structure information. For example, the Melbourne G-matrix in-medium nucleon-nucleon interaction [2], has successfully been used in the past few years for microscopic calculations of elastic scattering and inelastic scattering. When used with accurate structure information, the predicted scattering observables account very well for experimental data. Indeed, excellent agreement with data has been achieved in the analyses of elastic scattering of 65 and 201 MeV protons over a wide target range [2–5] including exotic nuclei [6,3,7]. Excellent agreement has also been achieved in describing inelastic scattering off light nuclei (^{12}C , ^{14}N , ^{16}O)[6,8] self-consistently, i.e. when using the same effective G-matrix for the transition operators and for the distorted waves in a distorted wave approximation (DWA). The accurate prediction (no adjusted parameter) of the differential cross sections and analysing powers for elastic and inelastic scattering with both natural parity and unnatural parity transitions, shows that all parts of the in-medium nucleon-nucleon (NN) interaction (central, spin-orbit and tensor) are well described. From these analyses, valuable information about nuclear excited states was extracted, such as particle-hole decomposition [9] or the degree of isospin mixing of some excitations [8].

In the present work, these fully microscopic analyses are extended to the case of inelastic proton scattering off heavy spherical nuclei for which mean-field and beyond the mean-field calculations are preferred to the shell-model approaches previously used for lighter nuclei. For this purpose, calculations of proton inelastic scattering off ^{208}Pb are presented. These calculations use structure information obtained from Self-Consistent RPA (SCRPA) calculations [10]. In the present context, Self-Consistency means that the same interaction (the Gogny D1S

interaction [11]) is used for calculating the mean field single particle states, and as the residual interaction in RPA calculations. The present work is a natural extension of our previous proton elastic scattering analysis [12] which uses the same structure information and the same microscopic effective interactions. In [12], the SCRPA+D1S description of the structure of doubly closed shell nuclei (when coupled with the Melbourne G-matrix) is shown to be accounting for both electron elastic scattering and medium energy proton elastic scattering, with comparable quality.

In this paper, we will first demonstrate that it is possible to describe inelastic proton scattering off doubly-closed shell heavy nuclei in a fully-microscopic framework (as described below) with the same accuracy as that obtained for scattering off light nuclei. For this purpose, predictions of differential inelastic cross-section for many excited states of ^{208}Pb with incident proton energy between 65 and 201 MeV will be discussed. Those calculations are performed within a single microscopic framework, with the same NA interaction and the same structure description for all studied transitions. No normalization process is involved and the knock-on exchange amplitude is treated exactly. Even though that structure framework has already been challenged through the comparison of charge transition densities [19], proton inelastic scattering calculations are sensitive to proton and neutron components of the RPA transition densities where both proton and neutron contribute on comparable footing. Moreover, the dominance of the isoscalar 3S_1 component of the nucleon-nucleon (NN) interaction [2] ensures that proton scattering observable are very sensitive to the neutron transition densities, which are hardly probed by electron scattering.

Our second motivation is to show that relevant conclusion on nuclear structure can only be obtained if the calculation of scattering observables is very accurate and involves no adjustment process. For this purpose, we compare our proton inelastic scattering calculations for high spin excitations to previous semi-phenomenological analyses which reveal some contradicting conclusions regarding the properties of those states. These high spin states have also been used as a test bed to assess the effect of “degraded” descriptions of those states on proton scattering observables. That study will highlight the sensitivity of those scattering observables to details of the nuclear structure of the target.

For the inelastic scattering of a nucleon off a zero-

spin ground state, the differential cross-sections are calculated with the DWBA expression of the transition amplitude: $\langle \chi^-(\mathbf{k}_f), n | V_{eff} | \chi^+(\mathbf{k}_i), \tilde{0} \rangle$ associated to excitations $|n\rangle$ of the target originally in the ground state $|\tilde{0}\rangle$. The V_{eff} interaction which generates the transition is the Melbourne G-matrix which includes central, tensor and spin-orbit components that are all energy and density dependent. The incoming $\chi^+(\mathbf{k}_i)$ and outgoing $\chi^-(\mathbf{k}_f)$ distorted waves entering the definition of DWBA matrix elements are obtained by solving the one-body Schrödinger equation describing the elastic scattering of a nucleon in a non-local optical potential. This microscopic optical potential is obtained by contracting the same interaction (the Melbourne G-matrix) on the target state which is described within the SCRPA+D1S framework for double-closed shell nuclei [12]. Note that, like in [12], our calculations use the true RPA correlated ground state $|\tilde{0}\rangle$ (including corrections for the quasi-boson approximation) and not the uncorrelated Hartree-Fock ground state. Excited states $|n\rangle = |NJ\Pi M\rangle$ of multipolarity, parity J, Π and spin projection M are then written as RPA excitations of $|\tilde{0}\rangle$:

$$\begin{aligned} |n\rangle &= |NJ\Pi M\rangle = \Theta_{NJ\Pi M}^+ |\tilde{0}\rangle \\ &= \sum_{ph \in (J\Pi)} \left[X_{ph}^N A_{JM\Pi}^+(p\tilde{h}) - Y_{ph}^N A_{J\bar{M}\Pi}(p\tilde{h}) \right] |\tilde{0}\rangle. \end{aligned} \quad (1)$$

The different quantities and operators appearing in this equation are defined in [12]. We recall that the X and Y amplitudes are obtained by solving the RPA equations for which the particle-hole interaction has been obtained in a self-consistent way, i.e. has been derived from the second derivative of the energy density functional obtained with the D1S interaction.

It is worth showing how structure information, the one-body transition densities, enters the DWBA matrix element. The fully antisymmetric formulation of the transition amplitudes involves local and non-local transition density matrices. The general expression of these density matrices elements is:

$$\begin{aligned} \rho_{\pm\frac{1}{2}, \pm\frac{1}{2}}^n(\mathbf{r}, \mathbf{r}', \boldsymbol{\sigma}, \boldsymbol{\sigma}') &= \\ \sum_{\alpha, \beta} \langle n | b_{\alpha, \pm\frac{1}{2}}^+ b_{\beta, \pm\frac{1}{2}} | \tilde{0} \rangle \phi_{\alpha}^*(\mathbf{r}) \chi_{\pm\frac{1}{2}}^{\frac{1}{2}*}(\boldsymbol{\sigma}) \phi_{\beta}(\mathbf{r}') \chi_{\pm\frac{1}{2}}^{\frac{1}{2}}(\boldsymbol{\sigma}'), \end{aligned} \quad (2)$$

where $\alpha \equiv (n_{\alpha}, l_{\alpha}, m_{\alpha})$, $\phi_{\alpha}(\mathbf{r}) = \langle \mathbf{r} | n_{\alpha} l_{\alpha} m_{\alpha} \rangle$ and $\chi_{\pm\frac{1}{2}}^{\frac{1}{2}}(\boldsymbol{\sigma}) = \langle \boldsymbol{\sigma} | \frac{1}{2}, \pm\frac{1}{2} \rangle$. The quantum numbers set $\alpha, \pm\frac{1}{2}$ refers to a Hartree-Fock single particle state for which the intrinsic spin and the angular momentum are uncoupled. Since we do not consider charge exchange reactions, we discard any dependence to the isotopic spin. The $\mathbf{r} = \mathbf{r}'$ case summed over the spin projections corresponds to the matter transition density which after angular integration reads:

$$\begin{aligned} \rho^n(r) &= \sum_{ph \in (J\Pi)} (X_{ph}^N + Y_{ph}^N) \phi_p^*(r) \phi_h(r) \\ &\quad \times C(j_p, j_h, J, L_p, l_h), \end{aligned} \quad (3)$$

where $C(j_p, j_h, J, L_p, l_h)$ is a simple geometric factor (see [10] for more details).

We present differential cross sections calculated with the method described above, namely with the Melbourne G-matrix folded with the SCRPA+D1S description of ground and excited states. Comparisons between our calculations and experimental data [13–18] are shown in Fig.1 for proton inelastic scattering off ^{208}Pb to the $3_1^-, 2_1^+, 4_1^+, 5_1^-$ and 5_2^- excited states, over a broad energy range. The overall agreement between theoretical calculations and data is very good. For the 3_1^- excited state, cross-sections are shown at four proton incident energies between 98 and 201 MeV, and comparisons between our calculations and the experimental data reveal good agreement both in shape and magnitude, which we interpret as the good quality of the Melbourne G-matrix (including its energy dependence) as well as the underlying SCRPA description of the 3_1^- state. This is also the case for the $2_1^+, 4_1^+$ and 5_2^- states for which we display only one incident energy. Previously [19], charge transition densities calculated with the SCRPA+D1 had been compared to experimental inelastic electron scattering data and have been shown to be very accurate in most cases (the results obtained with the D1S interaction are quasi-identical). The only exception to the overall good agreement, is the transition to the 5_1^- state for which the calculated cross-section magnitude at the forward angle peak is 50 % stronger than the experimental one. We also notice a slight overestimation for the transition to the 3_1^- states. These discrepancies had already been observed when charge transition densities were analyzed in [19], and that picture is consistent with our proton inelastic scattering analysis.

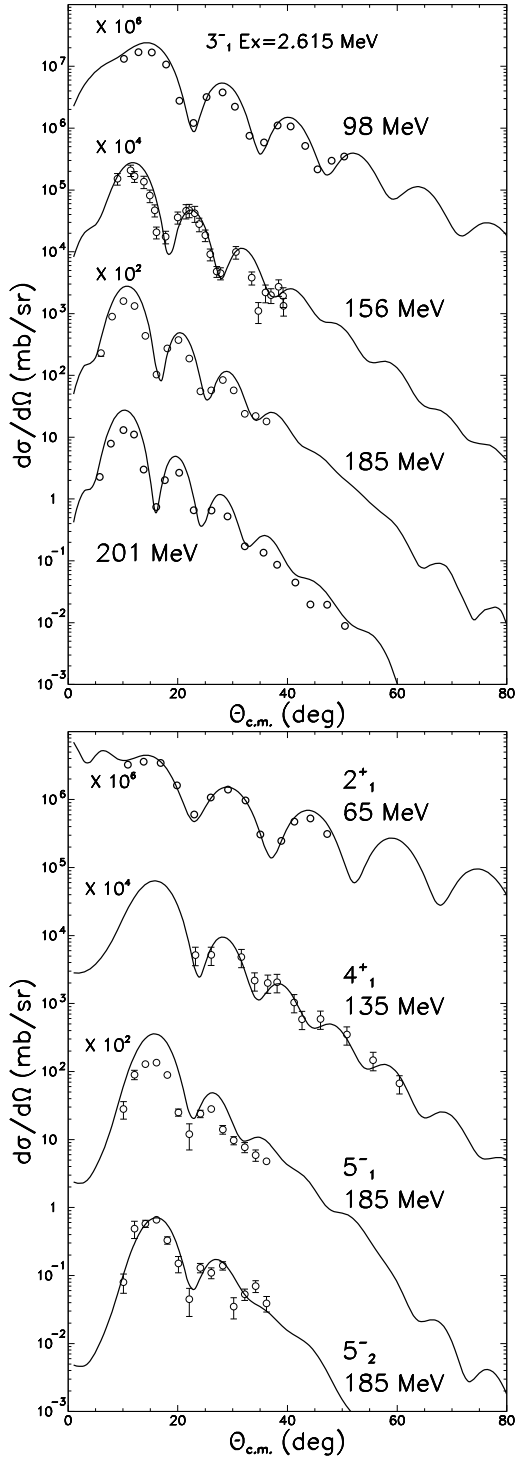


Fig. 1. Proton inelastic scattering off the 3_1^- (2.615 MeV), 2_1^+ (4.085 MeV), 4_1^+ (4.323 MeV), 5_1^- (3.197 MeV), and 5_2^- (3.708 MeV) excited states of ^{208}Pb . The incident energies are indicated on the plot. The results of the Melbourne+SCRPA+D1S calculations are displayed as solid curves and the experimental data [13–18] as symbols.

The same SCRPA+D1S transition densities have already been used [20] with a semi-phenomenological model to calculate high energy proton inelastic scattering to some discrete states of ^{208}Pb . The cross-sections obtained in this previous work needed sizable renormalization factors to account for the data, which led the authors to claim that the structure information used in those calculations is inaccurate. However, our results disagree with this conclusion and confirm the relevance of the SCRPA+D1S density matrices when be used in inelastic scattering calculations.

On Fig.2, we show a comparison between experimental inelastic differential cross-sections [21] and our calculations for transitions to high spin states, namely the 8_1^+ , 10_1^+ and 12_1^+ states. The solid lines represent the calculations performed with the Melbourne G-matrix folded with the SCRPA+D1S transition density matrices. Even for these high spin states, the agreement between the results of the G-folding calculation and the inelastic scattering data is excellent. Again, note that our calculations involve no normalization process.

It is worth pointing out that those high spin states have a correlated structure that must be described very accurately. First, the 8_1^+ state not only involves about 440 particle-hole pairs, but it also contains collectivity (materialized in the RPA description by “large” Y components) which cannot be ignored in our scattering calculations. That feature is illustrated on Fig.2, with a calculation performed after cancelling the Y components (dotted curve), which lies 30% below the complete calculation (full curve). An example of the nuclear structure accuracy needed for nucleon scattering calculations is given by the result obtained when seemingly minor particle-hole components are neglected. The dashed and dotted-dashed curves for the 8_1^+ transition correspond to the calculations which neglect configurations for which $Z < 0.01$ and $Z < 0.1$, respectively, with $Z = X, Y$. Keeping in memory the normalization of states, i.e. $N^2 = \langle n|n \rangle = \sum_{ph \in (J\Pi)} (X_{ph}^N)^2 - (Y_{ph}^N)^2 = 1$, these two truncations would seem to be good approximations since they correspond to a norm $N^2 = 0.957$ with 4 particle-hole components ($Z > 0.1$), and a norm $N^2 = 0.999$ with 39 particle-hole components ($Z > 0.01$). Yet, the effect of these truncations on the inelastic cross-sections is striking. Indeed, for the second truncation ($N^2 = 0.999$), the calculated cross section lies 50% below the complete calculation and for the first truncation ($N^2 = 0.957$), the

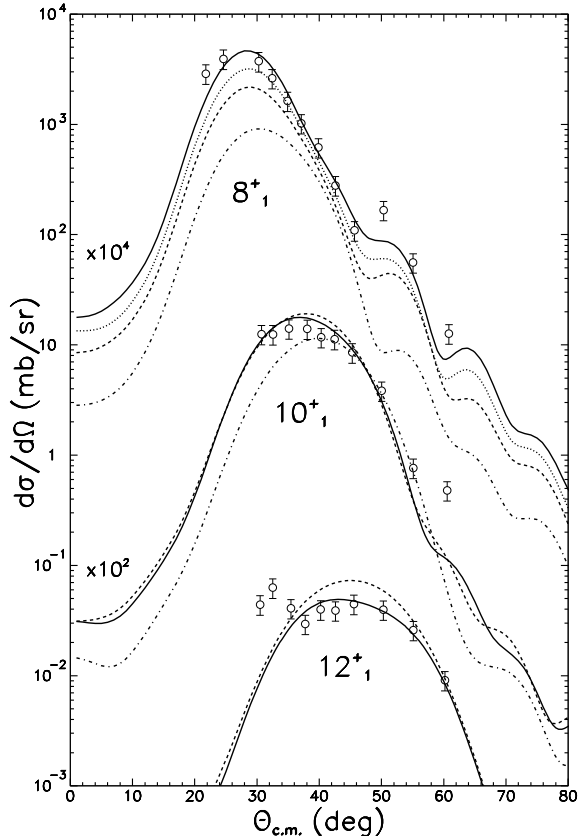


Fig. 2. Proton inelastic scattering off the 8_1^+ (4.610 MeV) 10_1^+ (4.895 MeV) and 12_1^+ (6.097 MeV) excited states of ^{208}Pb at 135.2 MeV. Experimental data are from [15]. The results of the Melbourne+SCRPA+D1S calculations are displayed as solid curves, the other curves are defined in the text.

calculated cross-section is five times lower than for the complete calculation, furthermore the shape of the distribution becomes incorrect.

Looking at the local proton and neutron transition densities associated with the 8_1^+ state (Fig. 3) reveals that the different truncations of the configuration space of the RPA components (canceled Y components or Z limited to components larger than 0.1 or 0.01) are clearly reflected in neutron (and, to a lesser extent, proton) transition densities. Although our proton scattering calculations involve the full non-local transition and current densities, the local densities shown in Fig. 3 can still help interpreting our proton scattering calculations with different configuration space truncations. Indeed, the differences between proton inelastic scattering calculations off the 8_1^+ state qualitatively track the changes of the associated neutron transition densities, as expected with a dominant 3S_1 NN interaction component in the G-matrix. The influence of the proton

transition density on proton inelastic scattering is not so easy to interpret, and is better understood when compared with electron inelastic scattering data (not shown). Yet, those differences highlight the effect of the long range correlation included in the SCRPA+D1S framework, materialized by seemingly minor Z components which nevertheless work coherently to produce strong effects in either local transition densities or in our inelastic proton scattering calculations.

The transition to the 10_1^+ state, exhibits a similar behaviour. This excited state presents weak collectivity, but 39 particle-hole components are still needed to accurately describe inelastic scattering. Yet, in previous analyses [22], this state was described with only three or four particle-hole configurations. On Fig. 2, the dashed line corresponds to a calculation for which the Z components lower than 0.1 have been cancelled. In this case, only three particle-hole components remain and the norm $N^2 = 0.984$ is still close to one. However the effect on calculated cross-sections is sizable since the “truncated” calculation lies 30% below the complete calculation and the cross section maximum is also shifted by 4 degrees. Looking at the associated local transition densities shows that truncating the configuration space produces almost no effect on the proton transition densities (not shown) while neutron (Fig. 3) densities exhibit changes which are qualitatively consistent with those exhibited by our proton inelastic scattering calculations.

We now consider the transition to the 12_1^+ state which is well-described by the single-particle-hole configuration $\nu(i_{9/2}, i_{13/2}^{-1})$. Figure 2 also displays a comparison between the calculation done with the Melbourne G-matrix (full curve) and the M3Y interaction [23] (dashed curve) for the transitions to the 10_1^+ and 12_1^+ states. While for the 10_1^+ transition, the calculation performed with the M3Y interaction is very close to that obtained with the Melbourne G-matrix, for the 12_1^+ transition, the inelastic cross section is overestimated by about 25%. The same result was obtained in a previous analyses using the M3Y interaction [22]. In order to explain this overprediction, that paper followed the line of a possible quenching effect for this particle-hole excitation that is clearly not needed in our analysis. This is a clear example for which DWBA analyses with different in-medium interactions can lead to contradicting conclusions on the underlying nuclear structure.

The inelastic scattering differential cross sections

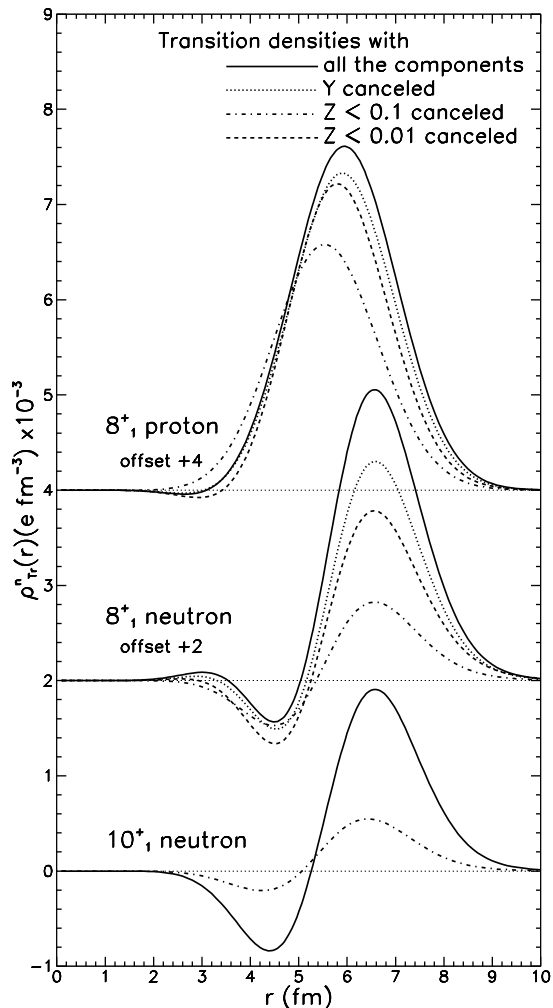


Fig. 3. Proton and neutron local transition densities to the 8_1^+ and 10_1^+ states calculated within the SCRPA+D1S framework with different truncations of configuration space.

of intermediate energy protons off ^{208}Pb was predicted for various excited states of diverse nature, using a fully microscopic parameter-free model. The density matrices used for the elastic and inelastic scattering calculations were obtained by SCRPA calculations using the D1S effective interaction. Those SCRPA densities were folded with the Melbourne G-matrix interaction to produce the microscopic optical potentials and transition matrix elements needed to describe scattering without any fitting of parameters to the data being described. Excellent agreement has been obtained for inelastic proton scattering up to the the 12_1^+ state for incident energies between 65 and 201 MeV. Proton scattering was shown to be a very good tool to precisely challenge the structure description of heavy spheri-

cal nuclei. This goal has been achieved because no phenomenological input or arbitrary renormalization process has been used in our microscopic model analysis, so that unambiguous conclusions on the structure of target nuclei can be drawn. Moreover, consistently with conclusions of previous electron scattering analyses [19], a disagreement is observed between SCRPA+D1S-based calculations and measurements for inelastic proton scattering in the case of the 5_1^- state. This is an example of both proton and electron scattering studies agreeing to pinpoint a deficiency in a description of nuclear structure. Finally, a precise description of nuclear structure is shown to be needed to account for inelastic scattering, since calculations using “degraded” structure information (canceled Y components or reduced configuration space) produce observables that do not match experimental data as well as the full calculations. This highlights the crucial role played by long range correlations in the description of the structure *and* scattering properties of the excited states of double-closed shell nuclei.

We have applied this approach to the study of discrete excitations and giant resonances in other double-closed shell or single-closed shell nuclei for which RPA is still a good approximation. The same framework can also be extended beyond discrete excitations, into the continuum, to analyze the pre-equilibrium emission associated with incoming nucleons. Works along these lines will be reported in upcoming papers.

Acknowledgments

This work was performed in part under the auspices of the U.S. Department of Energy by Lawrence Livermore National Laboratory under Contract DE-AC52-07NA27344.

References

- [1] D. Gupta, E. Khan and Y. Blumenfeld, Nucl. Phys. **A773**, 230 (2006).
- [2] K. Amos *et al.*, Adv. in Nucl. Phys. **25**, 275 (2000).
- [3] A. Lagoyannis *et al.*, Phys. Lett. **B518**, 27 (2001).
- [4] S. Karataglidis *et al.*, Phys. Rev. C **65**, 044306 (2002).
- [5] J. Klug *et al.*, Phys. Rev. C **67**, 031601(R) (2003).
- [6] S. Karataglidis *et al.*, Phys. Rev. Lett. **79**, 1447 (1997).
- [7] S. Karataglidis, Y.J. Kim, K. Amos, Nucl. Phys. **A793**, 40 (2007).
- [8] K. Amos, S. Karataglidis and Y.J. Kim., Nucl. Phys. **A762**, 230 (2005).

- [9] Y.J. Kim, K. Amos and S. Karataglidis, Nucl. Phys. **A779**, 82 (2006).
- [10] J. P. Blaizot et D. Gogny, Nucl. Phys. **A284**, 429 (1977).
- [11] J. F. Berger, M. Girod and D. Gogny, Comput. Phys. Commun. **63**, 365 ((1991)).
- [12] M. Dupuis, S. Karataglidis , E. Bauge, J.P. Delaroche and D. Gogny, Phys. Rev. C **73**, 014605 (2006).
- [13] Y.Fujita *et al.*, Phys. Rev. C **40**, 1595 (1989).
- [14] S. Kailas, Phys. Rev. C **35**, 2324 (1987).
- [15] G.S. Adams *et al.*, Phys. Lett. **B91**, 23 (1980).
- [16] V. Comparat *et al.*, Nucl. Phys. **A221**, 403 (1974).
- [17] A. Ingemarsson and B.Fagerstrom, Physica Scripta **13**, 208 (1976).
- [18] M. A. Hofstee *et al.*, Nucl. Phys. **A588**, 729 (1995).
- [19] J. Heisenberg *et al.*, Phys. Rev. C **25**, 2292 (1982).
- [20] V.E. Starodubsky and N. Hintz, J. Phys. G **21**, 803 (1995).
- [21] Y. Fujita *et al.*, Phys. Lett. **B91**, 27 (1980).
- [22] Y. Fujita *et al.*, Phys. Lett. **B247**, 219 (1990).
- [23] N. Anantaraman, H. Toki and G.F. Bertsch, Nucl. Phys. **A398**, 269 (1983).